



1 **Atmospheric Evolution of Emissions from a Boreal Forest Fire: The Formation of Highly-**
2 **Functionalized Oxygen-, Nitrogen-, and Sulfur-Containing Compounds**

3

4 Jenna C. Ditto¹, Megan He¹, Tori N. Hass-Mitchell¹, Samar G. Moussa², Katherine Hayden²,
5 Shao-Meng Li², John Liggi², Amy Leithead², Patrick Lee², Michael J. Wheeler²,
6 Jeremy J.B. Wenzell², Drew R. Gentner^{1,3,*}

7

8 ¹ Department of Chemical and Environmental Engineering, Yale University, New Haven, CT,
9 06511, USA; ² Air Quality Research Division, Environment and Climate Change Canada,
10 Toronto, Ontario M3H 5T4, Canada; ³ Solutions for Energy, Air, Climate and Health
11 (SEARCH), School of the Environment, Yale University, New Haven CT 0651, USA

12

13 * Correspondence to: drew.gentner@yale.edu

14

15 **Abstract**

16 Forest fires are major contributors of reactive gas- and particle-phase organic compounds
17 to the atmosphere. We used offline high resolution tandem mass spectrometry to perform a
18 molecular-level speciation of evolving gas- and particle-phase compounds sampled via aircraft
19 from a boreal forest fire in Saskatchewan, Canada. We observed diverse multifunctional
20 compounds containing oxygen, nitrogen, and sulfur (CHONS), whose structure, formation, and
21 impacts are understudied. The abundance of particle-phase CHONS species increased with
22 plume age, from 19% to 40% of the relative abundance of observed functionalized OA over the
23 first 4 hours of downwind transport. The relative contribution of particle-phase sulfide functional



24 groups increased with age from 4% to 40% of observed OA abundance, and were present in up
25 to 75% of CHONS compounds. The increases in sulfides were accompanied by increases in ring-
26 bound nitrogen, and both increased together with CHONS prevalence. A complex mixture of
27 intermediate- and semi-volatile gas-phase organic sulfur species was emitted from the fire and
28 depleted downwind, representing potential precursors to particle-phase CHONS compounds.
29 These results demonstrate CHONS formation from nitrogen/oxygen-containing biomass burning
30 emissions in the presence of reduced sulfur species, and highlight chemical pathways that may
31 also be relevant in situations with elevated levels of nitrogen and sulfur emissions from
32 residential biomass burning and fossil fuel use (e.g. coal), respectively.

33

34 **1 Introduction**

35 Forest fires are predicted to become increasingly prevalent and severe with climate
36 change (Abatzoglou and Williams, 2016; Barbero et al., 2015; Jolly et al., 2015). These fires are
37 an important and uncontrolled source of gas- and particle-phase compounds to the atmosphere,
38 including a complex mixture of gas-phase reactive organic carbon, primary organic aerosol
39 (POA), carbon monoxide, carbon dioxide, methane, ammonia, nitrogen oxides, and black carbon
40 (Akagi et al., 2011; Gilman et al., 2015; Hatch et al., 2015, 2018; Koss et al., 2018; Vicente et
41 al., 2013; Yokelson et al., 2013). Many of these emitted compounds are precursors to downwind
42 ozone and secondary organic aerosol (SOA) production (Ahern et al., 2019; Buysse et al., 2019;
43 Gilman et al., 2015; Hennigan et al., 2011; Lim et al., 2019).

44 Primary and secondary pollutants from biomass burning have important effects on air
45 quality locally, regionally, and continentally (Burgos et al., 2018; Colarco et al., 2004; Cottle et
46 al., 2014; Dreessen et al., 2016; Forster et al., 2001; Rogers et al., 2020; Val Martín et al., 2006),



47 and their impacts on human health and climate (e.g. via light absorbing brown and black carbon)
48 have been well documented (Forrister et al., 2015; Jiang et al., 2019; Liu et al., 2017; Di Lorenzo
49 et al., 2018; Reid et al., 2016; Sengupta et al., 2018; Wong et al., 2019). These health and climate
50 effects are sensitive to the elemental and structural composition of gas- and particle-phase
51 emissions and transformation products (Ditto et al., 2019; Hallquist et al., 2009; Nozière et al.,
52 2015). As a result, past studies have used online and offline mass spectrometry techniques to
53 characterize the chemical composition of fresh and aged biomass burning smoke and have
54 revealed a wide array of emitted hydrocarbons and oxygen-, nitrogen-, or sulfur-containing
55 functionalized species (Ahern et al., 2019; Bertrand et al., 2018; Gilman et al., 2015; Hatch et al.,
56 2015, 2018, 2019; Iinuma et al., 2010; Koss et al., 2018; Laskin et al., 2009; Yokelson et al.,
57 2013). However, the emissions and chemical transformations occurring in ambient biomass
58 burning plumes are extremely complex and despite previous measurements remain poorly
59 understood at the molecular-level.

60 In this study, we used an aircraft sampling system developed to collect offline gas- and
61 particle-phase organic compounds from a boreal forest fire. We examined the molecular-level
62 emissions and evolution of the forest fire plume with an unprecedented analysis of offline
63 aircraft samples using gas and liquid chromatography (GC/LC) with high resolution mass
64 spectrometry (MS), including tandem mass spectrometry (MS/MS). This degree of detailed
65 chemical speciation is important to advance knowledge of in-plume chemical pathways and
66 reaction products, long-distance transport, and fate of biomass burning products—all of which
67 will improve modeling capabilities and our understanding of the health and environmental
68 impacts of biomass burning smoke.



69 Specifically, the goals of this study were: (1) to perform a detailed speciation of gas- and
70 particle-phase organic compounds derived from the boreal forest fire in terms of elemental and
71 functional group composition, to assess changes in plume composition at the molecular-level as
72 the plume aged; and (2) to examine the evolution of oxygen-, nitrogen-, and sulfur-containing
73 (CHONS) compounds. These CHONS compounds made up 19-40% of functionalized organic
74 aerosol here and have been observed at other ambient sites (e.g. 9-11% (Ditto et al., 2018)),
75 though little is known about their structures or formation mechanisms. Using our observations of
76 gas-phase sulfur species, we also identified possible precursors and reaction pathways involved
77 in the formation of these CHONS compounds.

78

79 **2 Materials and Methods**

80 On June 25th, 2018, two aircraft research flights were conducted by Environment and
81 Climate Change Canada as part of their Air Pollution research program. These flights sampled
82 two boreal forest wildfire smoke plumes originating near Lac LaLoche in northern
83 Saskatchewan, Canada (Figure S1). The region is dominated by pine and spruce trees (Canada's
84 National Forest Inventory, 2020). Gas- and particle-phase samples were collected from the
85 National Research Council of Canada's Convair-580 research aircraft for analysis with offline
86 high resolution mass spectrometry, alongside many other measurements (Supporting Information
87 S1-S2). The aircraft flew the same straight line tracks at multiple altitudes through the smoke
88 plumes, which when stacked created a virtual screen intercepting the plumes, at each of five
89 downwind locations (flight design similar to those previously reported (Li et al., 2017; Liggio et
90 al., 2016)); screen 1 was ~10 km from the fire with screens 2-4 following the plumes downwind,
91 and screen 5 intercepting the plumes after they had passed over several major surface and in-situ



92 mining oil sands facilities (Figure S1). The samples discussed here were collected across both
93 plumes to ensure that enough mass was present to surpass the mass spectrometer's detection
94 limit. Based on satellite information and aircraft measurements at the start of sampling (i.e.
95 screen 1), the fire was a low-intensity surface fire with smoldering conditions; aircraft
96 measurements indicated a modified combustion efficiency of 0.90 ± 0.40 for both plumes.

97 Combined gas- and particle-phase samples were collected onto custom adsorbent tubes
98 packed with high-purity quartz wool, glass beads, Tenax TA, and Carbopack X (Sheu et al.,
99 2018). Samples were collected along screens 1-4 in Figure S1 (no adsorbent tubes collected at
100 screen 5) via an external pod mounted under the wing of the aircraft which included remote
101 switching between adsorbent tubes at various transect altitudes and online measurements of
102 temperature, pressure, and flow (Supporting Information S1, Figure S2). While particles were
103 not explicitly filtered out (to reduce losses of lower volatility gases onto upstream surfaces), we
104 assumed that the compounds measured in the adsorbent tubes below C_{22} - C_{23} were primarily in
105 the gas-phase based on (1) significant undersampling for particles at the adsorbent tube inlet,
106 since the adsorbent tube sampling flow rate was a factor of ~ 4 lower than its corresponding
107 isokinetic flow rate, resulting in a significant divergence of particles away from the inlet during
108 sampling; (2) partitioning theory and average in-plume organic aerosol (OA) concentrations of
109 18 - $22 \mu\text{g}/\text{m}^3$ across adsorbent tube sampling periods for screens 1-4 (concurrently measured by
110 an aerosol mass spectrometer (AMS) onboard the aircraft, Supporting Information S1, S3, Table
111 S2). As such, we limited the following adsorbent tube data analysis to compounds in the C_{10} - C_{25}
112 range to focus on intermediate-volatility and semivolatile (I/SVOCs) compounds predominantly
113 in the gas-phase.



114 Dedicated particle-phase samples were collected on 47 mm PTFE filters (2.0 μm pore;
115 Pall Corporation) from a sampling manifold in the cabin containing six independent anodized
116 aluminum filter holders. The filters were sampled behind an isokinetic inlet with a size cutoff of
117 approximately 2.5 μm . One filter sample was collected per screen for screens 1-5 shown in
118 Figure S1.

119 All adsorbent tubes were analyzed using a GERSTEL Thermal Desorber TD 3.5+ with
120 gas chromatography (Agilent 7890B GC), atmospheric pressure chemical ionization (APCI), and
121 quadrupole time-of-flight mass spectrometry (Agilent 6550 Q-TOF), similar to past work (Khare
122 et al., 2019). For adsorbent tubes, the APCI was operated in positive ionization mode. The Q-
123 TOF was operated in MS mode (i.e. TOF data collection, hereafter “GC-APCI-MS”). Adsorbent
124 tube data were processed primarily via a targeted approach for C_xH_y , $\text{C}_x\text{H}_y\text{O}_1$, and $\text{C}_x\text{H}_y\text{S}_1$
125 compounds using custom Igor Pro code (Supporting Information S2-S3).

126 Filter samples were extracted in methanol (Ditto et al., 2018). Samples were analyzed via
127 liquid chromatography (Agilent 1260 LC) with electrospray ionization (ESI) and the same Q-
128 TOF. For filters, the ESI source was operated in both positive and negative ionization mode, and
129 the Q-TOF was operated in both MS mode (i.e. TOF data collection, “LC-ESI-MS”) and MS/MS
130 mode (i.e. tandem mass spectral data collection, “LC-ESI-MS/MS”) (Ditto et al., 2018, 2020).
131 Filter extracts were also analyzed using GC-APCI-MS in positive ionization mode. Filter data
132 from LC-ESI-MS, LC-ESI-MS/MS, and GC-APCI-MS were analyzed with a non-targeted
133 approach, using Agilent Mass Hunter, SIRIUS with CSI:FingerID, and custom R code
134 (Supporting Information S2-S3) (Ditto et al., 2018, 2020). All peaks that passed strict QC/QA
135 were assigned molecular formulas, with candidate formulas limited to 20 oxygen, 3 nitrogen,
136 and/or 1 sulfur atom(s). Note that these compound classes are discussed here without subscripts.



137 Additional details on these methods, including an analysis of total mass analyzed from
138 filters and adsorbent tubes, are discussed in Supporting Information S1-S5, with a methods
139 summary in Figure S3.

140

141 **3 Results and Discussion**

142 3.1 Evolution of organic aerosol elemental composition and functionality with plume age

143 Our analysis of functionalized OA showed several compositional trends in the evolving
144 boreal forest fire smoke plume (screens 1-4) and exhibited marked changes after emissions from
145 the oil sands facilities were mixed with the forest fire plume (screen 5). Here, we focused on the
146 forest fire plume in screens 1-4. We observed a diverse elemental composition in functionalized
147 OA across oxygen-, nitrogen-, and/or sulfur-containing compound classes (Figure 1A-1B, Figure
148 S5). This included compounds containing oxygen (CHO), such as common biomass burning
149 tracers and their isomers (e.g. levoglucosan, Supporting Information S2); as well as oxygen- and
150 nitrogen- containing compounds (CHON); oxygen- and sulfur-containing compounds (CHOS);
151 reduced nitrogen-containing compounds (CHN); reduced nitrogen- and sulfur-containing
152 compounds (CHNS); as well as compounds containing oxygen, nitrogen, and sulfur (CHONS).

153 There was a continual decrease in the relative abundance of particle-phase CHO
154 compounds in measured functionalized OA across screens 1-4, accompanied by a consistent
155 relative increase in CHON and CHONS compounds (Figure 1B). Notably, the relative abundance
156 of CHONS compounds increased from 19 to 40% of measured functionalized OA abundance
157 from screens 1-4. These trends were similar in the carbon monoxide-normalized abundance of
158 these compound classes (Figure S5C), where CHO generally decreased from screens 1-4, while
159 CHONS and CHON generally increased, suggesting that CHONS compounds were possibly



160 formed from CHO, CHN, and/or CHON precursors existing across both gas- and particle-phases
161 in the plume (proposed chemistry discussed in Section 3.5). From MS/MS, these evolving CHO,
162 CHN, CHON, and CHONS compounds were often comprised of variable combinations of
163 hydroxyls, ethers (e.g. primary emissions from forest fires like methoxyphenols and similar
164 structures), amines, imines, cyclic nitrogen features (consistent with past laboratory observations
165 of biomass burning emissions (Laskin et al., 2009; Lin et al., 2018; Liu et al., 2015; Updyke et
166 al., 2012)), and sulfides.

167

168 3.2 Detailed speciation of CHONS compounds in functionalized OA

169 While some individual CHONS functional groups contained grouped oxygen, nitrogen,
170 and sulfur atoms (e.g. sulfonamides), the majority of CHONS compounds had a combination of
171 multiple separate oxygen-, nitrogen-, and/or sulfur-containing functional groups (Figure 2A-2B).
172 Sulfide groups were important contributors to CHONS compounds (Figure 2B) and showed a
173 notable increase in relative contribution to the overall functional group distribution, from 4-40%
174 of measured compound abundance across screens 1-4 (Figure 1C). Their increasing relative
175 contribution to CHONS compounds with plume evolution was even more pronounced—by
176 screen 4, the sulfide functional group was present in 75% of detected CHONS compound
177 abundance (Figure S7A). Here, we focused on the presence of sulfides in CHONS compounds
178 because most of the observed particle-phase sulfides occurred as part of CHONS species (71%),
179 while a smaller fraction occurred as CHOS (21%) or CHNS (8%) (Figure 3A).

180 To explore possible precursors and formation pathways for these particle-phase sulfide-
181 containing CHONS species, we used MS/MS to identify nitrogen-containing functional groups
182 that co-occurred with sulfides. In CHONS compounds, most sulfides co-occurred with cyclic



183 nitrogen (36%), amine (32%), or imine features (43%) (Figure 3B). The prevalence of sulfide
184 and cyclic nitrogen features in the measured functionalized OA increased together screen-to-
185 screen, and increased together with the rising proportion of CHONS compounds (Figure 3C).
186 While sulfides often co-occurred with amines or imines and while amines and imines were
187 prevalent in all 4 screens (Figure 1C), there was no relationship between amines or imines and
188 the increasing contribution of CHONS compounds to measured functionalized OA (Figure S7B).

189 The sulfide substructures observed via MS/MS often contained linear carbon chains or
190 phenyl groups bonded to the sulfur atom (Figure 3C inset). Thus, we hypothesize that precursors
191 with similar reduced sulfur-containing structures reacted with cyclic nitrogen-containing species
192 to form the observed sulfide-containing CHONS compounds, which increased in prevalence with
193 plume age (precursors discussed in Section 3.3, potential chemical pathways discussed in Section
194 3.5).

195 CHONS compounds were predominantly SVOCs in screens 1-4 (i.e. 89% of CHONS ion
196 abundance, Figure 2C, Figure S8), suggesting that these compounds were formed from lighter
197 gas-phase species. In contrast, with the influence of the oil sands facilities in screen 5, 68% of
198 CHONS compounds were extremely low volatility organic compounds (ELVOCs), though
199 CHONS made up only 2% of functionalized OA at screen 5. CO-normalized abundances of
200 functionalized OA in each particle-phase volatility bin (i.e. IVOC, SVOC, LVOC, ELVOC,
201 computed using LC-derived molecular formulas with the Li et al. parameterization (Li et al.,
202 2016)) increased with plume age, but the relative contribution of SVOCs increased from 37% to
203 58% while the relative contribution of IVOCs dropped from 38% to 20%, potentially due to
204 oxidation reactions that formed SVOCs and/or due to evaporation (Figure S9). These particle-
205 phase IVOCs consisted predominantly of CHO, CHN, and CHON ($O/N < 3$) compounds, which



206 are possible non-sulfur containing precursors to the observed CHONS species. Fragmentation of
207 particle-phase L/ELVOC compounds also could have contributed to some of the observed SVOC
208 mass, but the increasing total abundance across all volatility bins with plume age supports the
209 idea that these compounds were predominantly formed from more volatile precursors (e.g.
210 I/SVOCs).

211

212 3.3 Targeted search for CHONS precursors in the gas-phase

213 To investigate possible gas-phase I/SVOC precursors to the observed sulfide-containing
214 CHONS compounds, we performed a targeted search for each adsorbent tube sample across all
215 C_{10} - C_{25} $C_xH_yS_1$ species with the equivalent of 0-15 double bonds and/or rings (i.e. $C_xH_{2x+2}S_1$ -
216 $C_xH_{2x-28}S_1$, Figure 4A, Figure S10). We observed a distribution of $C_xH_yS_1$ compounds and their
217 isomers; based on the high mass resolution and high mass accuracy molecular formulas from
218 targeted GC-APCI-MS analysis, 27% of $C_xH_yS_1$ compounds were fully saturated (i.e. $C_xH_{2x+2}S_1$)
219 and 25% contained the equivalent of 4-6 double bonds and/or rings (i.e. $C_xH_{2x-6}S_1$ - $C_xH_{2x-10}S_1$),
220 which included single ring aromatics. We focused on these sulfur-containing gases as candidate
221 precursors to the observed sulfide-containing CHONS compounds as they contained sulfur
222 substructures with linear carbon chains or phenyl groups, similar to those observed on CHONS
223 compounds via MS/MS OA analysis (Figure 3C inset, Figures S10-S11). However, we also
224 observed contributions from other sulfur-containing structures (e.g. with the equivalent of 1-3
225 double bonds and/or rings, in Figure 4A), which could also be involved as precursors.

226 The observed gas-phase C_{10} - C_{25} $C_xH_yS_1$ compounds were emitted by the fire and likely
227 also evaporated from the particle-phase during early plume dilution. Gas-phase C_{10} - C_{25} $C_xH_yS_1$
228 concentrations increased relative to carbon monoxide from screen 1 to 2, then steadily decreased



229 with plume age (Figure 4B, Figure S12A). This suggests the emission and/or evaporation of
230 $C_xH_yS_1$ compounds between screens 1 and 2, and subsequent participation in plume chemistry
231 from screens 2 to 4.

232 Similar OA evaporation with plume dilution has been observed in many past studies
233 (Ahern et al., 2019; Garofalo et al., 2019; Hennigan et al., 2011; Lim et al., 2019). However, to
234 better understand the dynamics of these sulfur-containing compounds, we compared their
235 concentrations to concentrations from a targeted search of adsorbent tube gas-phase compounds
236 that included C_{10} - C_{25} aliphatic and aromatic C_xH_y and $C_xH_yO_1$ species. Overall, C_xH_y and $C_xH_yO_1$
237 compound classes dominated the observed C_{10} - C_{25} compounds (Figure 4B, Figure S12B), with
238 61% C_xH_y , 36% $C_xH_yO_1$, and just 3% $C_xH_yS_1$ on average. C_xH_y and $C_xH_yO_1$ concentrations
239 generally increased with plume age (Figure 4B) and included many known compound types (e.g.
240 monoterpenes, aromatics, hydroxyls, carbonyls (Akagi et al., 2011; Andreae, 2019; Gilman et al.,
241 2015; Hatch et al., 2015, 2019; Koss et al., 2018)). This suggests the direct emission of these
242 gas-phase compounds from the fire (observed at screen 1) and evaporation from the particle-
243 phase as the plume evolved, as well as formation of $C_xH_yO_1$ via oxidation of C_xH_y compounds.
244 AMS measurements of total OA concentrations provided supporting evidence of OA
245 evaporation; the ratio of AMS OA concentration to CO decreased by 7% from screen 1 to 2
246 (corresponding to an AMS OA/CO ratio of -0.0044 or a decrease in OA concentration of -2.3
247 $\mu\text{g}/\text{m}^3$), while the ratio of total gas-phase C_xH_y , $C_xH_yO_1$, and $C_xH_yS_1$ concentration to CO
248 increased by 55% (corresponding to a total gas-phase concentration/CO ratio of 0.022 or an
249 increase in gas-phase concentration of $7.0 \mu\text{g}/\text{m}^3$, Table S3). While not the focus of the analytical
250 approaches applied in this study, to further substantiate the observation of OA evaporation, we
251 performed the same targeted analysis of C_{10} - C_{25} C_xH_y , $C_xH_yO_1$, and $C_xH_yS_1$ compounds in the



252 particle-phase filter sample extracts analyzed via GC-APCI-MS and observed a similar decrease
253 in concentration from screen 1 to 2. However, these filter measurements (even with APCI
254 ionization) were not geared towards C_xH_y and $C_xH_yS_1$ measurements due to possible solubility
255 limitations in the extraction solvent (Supporting Information S4). Direct thermal desorption of
256 adsorbent tubes or filters with APCI ionization would be better suited for these C_xH_y and $C_xH_yS_1$
257 measurements (as performed in this study with adsorbent tubes).

258 Also, as discussed in *Materials and Methods*, the observed semivolatile compounds
259 below $\sim C_{22}$ - C_{23} existed primarily in the gas-phase, while larger compounds actively partitioned
260 to and equilibrated with the particle-phase, further corroborating the possibility of contributions
261 from both direct gas-phase emissions and gases from OA evaporation (Supporting Information
262 S3, Table S2). In contrast to C_xH_y concentrations, $C_xH_yS_1$ concentrations dropped markedly after
263 screen 2 despite similarities in the volatility distribution of C_xH_y and $C_xH_yS_1$ I/SVOCs in their
264 respective complex mixtures (Figure 4A, Figures S10 and S13). This difference shows that the
265 observed $C_xH_yS_1$ I/SVOCs were removed (possibly by chemical reactivity) relatively more
266 rapidly than C_xH_y , thus supporting their potential contribution to CHONS formation.

267 In addition to the C_{10} - C_{25} $C_xH_yS_1$ compounds measured in the adsorbent tubes, smaller
268 sulfur-containing compounds could have also acted as CHONS precursors, like those identified
269 by the onboard proton transfer reaction-mass spectrometer (PTR-ToF-MS). While dimethyl
270 sulfide (DMS, previously observed in biomass burning smoke (Andreae, 2019)) was often below
271 its instrument limit of detection, both dimethyl and diethyl sulfide showed good correlation with
272 acetonitrile, a well-known biomass burning product (Andreae, 2019), in the smoke plume during
273 screen 1 ($r \sim 0.95$, Figure S12C). This suggests that these compounds were co-emitted by the fire
274 (Akagi et al., 2011; Andreae, 2019; Hatch et al., 2015; Koss et al., 2018).



275 3.4 Investigating possible origins of gas-phase sulfur compounds

276 The gas-phase sulfur-containing compounds observed in the plume were emitted from the
277 smoldering fire. However, their origins are uncertain, since the broader range of sulfur species
278 found here (Figure 4A, Figures S10-11) has not yet been reported; many of the compounds in the
279 complex sulfur-containing mixture measured here were outside the detection range or
280 measurement capability of previously employed methods (Hatch et al., 2015; Khare et al., 2019;
281 Koss et al., 2018; Sekimoto et al., 2018). Here, we explore two potential origins of these gas-
282 phase sulfur-containing precursors to the observed particle-phase CHONS compounds: the
283 biomass fuel itself and the deposition of sulfur species from anthropogenic/industrial operations.

284 *Fuel:* In past studies, emissions of sulfur-containing organic compounds were typically
285 minor compared to-oxygen- or nitrogen-containing compounds, and the relative balance of
286 oxygen-, nitrogen-, or sulfur-containing compound emissions was typically proportional to fuel
287 content (Hatch et al., 2015; Ward, 1990). The estimated N:S ratio for boreal forest fuel near the
288 fire was ~10:1 (Huang and Schoenau, 1996), which was similar to the average N:S ratio from a
289 non-targeted search for nitrogen- and sulfur-containing I/SVOCs from the adsorbent tube
290 samples in this study of $(8.1 \pm 4.8):1$. Sulfur is an essential nutrient in plants, and can be taken up
291 from soil (as sulfate) or from the atmosphere via deposition (as SO₂ and sulfate) (Aas et al.,
292 2019; Gahan and Schmalenberger, 2014; Leustek, 2002). Both SO₂ and sulfate are metabolized
293 in plants to yield a variety of compounds critical to plant functions including cysteine and a
294 range of other sulfur- (and oxygen- and nitrogen-) containing compounds (Leustek, 2002). In
295 addition, disulfide bonds contribute to plant protein structure, and these bonds are known to
296 cleave and form thiols (Gahan and Schmalenberger, 2014; Leustek, 2002; Onda, 2013). Sulfur-
297 containing compounds like these may have been emitted during the fire, along with other known



298 sulfur products from boreal fuels (e.g. DMS, thiophenes (Akagi et al., 2011; Hatch et al., 2015;
299 Koss et al., 2018; Landis et al., 2018)).

300 *Deposition:* While sulfur can be naturally occurring (e.g. Leustek, 2002), it is also
301 associated with anthropogenic activities (e.g. transportation, power generation, industry, etc.).
302 This implies that a portion of the sulfur in the forest fire emissions could have originated from
303 sulfur deposited via such anthropogenic activities. The closest large anthropogenic sulfur source
304 to the fire location was the oil sands mining region north of Fort McMurray, Alberta, which was
305 approximately 150 km away and which contained known SO₂ emitters (Liggio et al., 2017;
306 McLinden et al., 2016). Regional concentrations of SO₂ or other sulfur species from these nearby
307 industrial activities could have led to accumulated deposition of inorganic and/or organic sulfur
308 compounds over time, though it is uncertain how much of this deposited sulfur would have been
309 taken up and transformed by vegetation (vs. accumulated) due to sulfur uptake and assimilation
310 regulatory pathways in plants (Davidian and Kopriva, 2010). This possible accumulated
311 deposition may have acted as a reservoir of sulfur to be emitted during fires via the re-
312 volatilization of deposited compounds, in addition to the evaporation of typical sulfur
313 metabolites or the formation of sulfur-containing combustion by-products. This hypothesis is
314 consistent with recent deposition measurement and modelling results for the region, which
315 indicated that sulfur deposition from the oil sands potentially impacted areas downwind,
316 including the region where this fire occurred (Makar et al., 2018). Interestingly, lichen and
317 spruce trees, which are prominent in the region of the fire discussed here, have been reported to
318 accumulate sulfur from SO₂ in regions near large industrial SO₂ sources (Meng et al., 1995;
319 Nyborg et al., 1991). Also, past studies have reported enhancements in sulfate (as well as nitrate
320 and ammonium) aerosols from biomass burning in areas with urban influence (Fenn et al., 2015;



321 Hecobian et al., 2011; Hegg et al., 1987). Inorganic aerosol components from both urban (e.g.:
322 Edmonton, Alberta) and industrial (e.g. oil sands) sources could deposit in the area surrounding
323 the emissions source along with an organic phase, which we postulate could contain a range of
324 sulfur-containing species including the $C_xH_yS_1$ compounds shown here. However, further work is
325 needed to disentangle the contribution of natural vs. anthropogenic sulfur to functionalized OA
326 from biomass burning.

327

328 3.5 Potential reaction pathways leading to sulfides in CHONS from sulfur precursors

329 A number of potential reactions involving sulfur-containing precursors, often thiols (R-
330 SH), may have contributed to the formation of the observed sulfide functional groups in particle-
331 phase CHONS compounds (Figure S14). On average, our gas-phase measurements showed a
332 27% contribution of fully saturated sulfur-containing hydrocarbons (i.e. $C_xH_{2x+2}S_1$, Figures S10-
333 11). It is likely that some fraction of the sulfur compounds observed in the gas-phase adsorbent
334 tube measurements (e.g. the compounds identified as $C_xH_{2x+2}S_1$) and in PTR-ToF-MS
335 measurements (e.g. dimethyl sulfide, diethyl sulfide) were thiols, but the distinction between
336 sulfide and thiol isomers was challenging without specific internal standards.

337 In some of the following possible reactions, a thiol interacts with a non-sulfur precursor
338 to yield a sulfide-containing compound. The non-sulfur precursor (in the gas- or particle-phase)
339 may have contained O and N atoms, thus yielding a CHONS compound immediately after
340 participating in one of the proposed reactions. Alternatively, the newly formed sulfide-containing
341 compound may have undergone subsequent, separate reactions with CHO, CHN, and/or CHON
342 compounds (in the gas- or particle-phase) to form the observed sulfide-containing CHONS
343 species. Here, we focused on possible reactions that could have contributed the sulfide group to



344 these oxygen- and/or nitrogen-containing compounds (known emissions from forest fires, as
345 discussed above). Earlier, we postulated that because most of the observed CHONS compounds
346 were SVOCs, these compounds were predominantly formed by reactions of more volatile gas-
347 phase I/SVOCs, and thus we examined potential gas-phase precursors in the C₁₀-C₂₅ range.
348 However, it is uncertain whether these sulfide-forming and CHONS-forming reactions occurred
349 in the gas-phase with subsequent partitioning to the particle-phase, heterogeneously, or in a
350 combination of separate gas- and particle-phase chemistry. We suggest some possible sulfide-
351 forming reactions here, yet we note that these proposed reactions are likely not comprehensive.
352 Further work to elucidate the chemistry driving this sulfide and CHONS formation is needed.

353 Some possible reactions include: (1) thiol-ene reactions, where a thiol reacts with an
354 alkene (or alkyne), which can form carbon-sulfur bonds (Lowe, 2010). Alkenes are known to be
355 prominent in emissions from boreal fires (Gilman et al., 2015; Hatch et al., 2015), and we
356 observed similar structures in our gas-phase samples that likely included alkenes, cyclic alkanes,
357 and/or monoterpenes (Figure S13). (2) Thiol reactions with carbonyls, which can form
358 hemithioacetals that subsequently dehydrate in the atmosphere to yield sulfides (Jencks and
359 Lienhard, 1966). This reaction is similar to the formation of enamines from carbonyls and
360 dimethyl amine via the formation and subsequent dehydration of a carbinolamine, which has
361 been shown to occur in ambient conditions (Duporté et al., 2016, 2017). (3) Thiol reactions with
362 alcohols, which can form sulfides. These reaction rates are low in the absence of catalysts and
363 require relatively high temperature to occur (i.e. 200-450°C; temperatures that are relevant very
364 close to the fire but unlikely in the rapidly cooling plume (Mashkina, 1991)). (4) Another
365 possibility is that a radical intermediate product formed during atmospheric oxidation of DMS
366 (e.g. the methylthiomethyl radical (CH₃SCH₂•) from OH•-driven hydrogen abstraction of DMS



367 (Barnes et al., 2006)) interacted with CHN and CHON precursors to yield the sulfide-
368 containing CHONS products. However, the concentrations of the methylthiomethyl radical and
369 similar radicals from other small sulfide precursors would likely be lower than those of other
370 major drivers of in-plume radical chemistry (e.g. O₂, NO_x, etc.), thus making this reaction
371 pathway less likely to contribute.

372 Based on our observations of these sulfide-containing products across flight screens, the
373 overall timescales for these sulfide-forming reactions was likely approximately 1 hour (or less).
374 For the literature reactions referenced above, reaction timescales ranged from minutes to hours in
375 laboratory experiments, but extrapolation to timescales in an ambient smoke plume is uncertain.
376 Specifically, it is challenging to compare to predicted timescales for the proposed reactions
377 without knowing the exact structure/identities of the reactants or the possible role of other key
378 modifying factors in the smoke plume (e.g. aerosol pH, presence of water).

379

380 **4 Implications & Conclusions**

381 In this work, we performed the first high resolution tandem mass spectrometry analysis of
382 an evolving smoke plume from a smoldering boreal forest fire. The results show clear evidence
383 of gas-phase sulfur-containing emissions from the fire, and an increasing contribution from
384 particle-phase CHONS compounds with sulfide functional groups as the plume evolved.
385 Together, these results suggest the emission of gas-phase sulfur-containing compounds from the
386 fire and subsequent gas- and/or particle-phase chemistry that produced multifunctional sulfide-
387 containing CHONS compounds.

388 Sulfide functional groups in air have been reported at a range of U.S. locations from
389 urban inland (1-7% sulfides), urban coastal (5-12% sulfides), and remote forested (7% sulfides),



390 and on average, sulfides comprised 28% of sulfur-containing functional groups at these sites
391 (Ditto et al., 2020). However, in past work, 53% of these sulfides were present in CHOS
392 compounds, while 34% were CHONS, and 13% were CHNS (in contrast to 21%, 71%, and 8%
393 in this study, respectively). Notably, at a Northeastern U.S. coastal site where there were several
394 pollution events linked to long distance transport of biomass burning smoke during field
395 sampling (Rogers et al., 2020), 70-90% of sulfides were present in CHONS compounds (Ditto et
396 al., 2020), similar to the distribution of sulfides discussed here (Figure 3A).

397 These results, along with past observations, highlight that this type of chemistry and these
398 types of reaction products may be relevant to other regions where concentrations of nitrogen and
399 sulfur-containing precursors are high, such as in developing regions, emerging economies, or
400 megacities where residential biomass burning is common and coincident with extensive use of
401 sulfur-containing fossil fuels (e.g. coal). CHONS compounds have been reported in similar
402 regions in past studies (Lin et al., 2012; Pan et al., 2013; Song et al., 2019; Wang et al., 2017a,
403 2016, 2017b). Their formation is potentially important since the presence of sulfur (including in
404 sulfide functional groups), oxygen, and nitrogen can affect the glass transition temperature and
405 thus the phase state (e.g. solid, semi-solid, liquid), as well as the mixing state (e.g. well-mixed,
406 phase-separated) of particles (DeRieux et al., 2018; Ditto et al., 2019; Van Krevelen and Te
407 Nijenhuis, 2009). These physical properties may influence particles' chemical reactivity and thus
408 persistence in the atmosphere, along with their transport and deposition, all of which contribute
409 to the health and environmental impacts that communities and ecosystems experience from OA
410 exposure. Future work to identify prominent functional groups in CHONS species in regions
411 with high CHONS concentrations will help elucidate the formation chemistry of these
412 functionalized compounds, and understand and mitigate their associated impacts.



413 **Acknowledgments**

414 The authors acknowledge GERSTEL for their collaboration with the TDU 3.5+, used to run the
415 adsorbent tubes discussed in this study. We thank Environment and Climate Change Canada and
416 National Research Council technical teams for their help in the construction and maintenance of
417 cartridge sampling systems, specifically Tak Chan (Environment and Climate Change Canada)
418 for help collecting samples. We also thank Jo Machesky (Yale) for help running adsorbent tube
419 samples, Joe Lybik (Yale) for help packing adsorbent tubes, and Daniel Thompson (Natural
420 Resources Canada) for informative discussion. J.C.D., M.H., T.H-M., and D.R.G. acknowledge
421 support from National Science Foundation grant AWD0001666. We also acknowledge funding
422 from the Air Pollution (AP) program of Environment and Climate Change Canada. The flights
423 discussed in this study were embedded within a 2018 oil sands monitoring intensive campaign,
424 and the oil sands monitoring program is acknowledged for enabling the flights.

425

426 **Author Contributions**

427 J.C.D. ran samples, processed filter data, compiled and interpreted results. M.H. processed
428 adsorbent tube data. T.H-M. contributed to MS/MS analysis. S.G.M., K.H., J.L., and D.R.G.
429 collaborated on data interpretation. K.H. collected and processed AMS data. A.L. collected and
430 processed PTR-ToF-MS data. S.-M.L. designed the aircraft adsorbent tube collection system.
431 P.L. and J.J.B.W. implemented the wing pod design. P.L. prepared the wing pods for collection
432 and J.J.B.W. and J.L. collected the adsorbent tube samples. M.J.W. and J.L. designed the filter
433 collection system. M.J.W. and K.H collected filter samples. S.-M.L., K.H., and J.L. designed the
434 aircraft sampling study. J.C.D. and D.R.G. wrote the manuscript, with input from all co-authors.

435



436 **Competing Interests**

437 The authors declare that they have no conflict of interest.

438

439 **Code and Data Availability**

440 Code and data are available upon request.

441

442 **References**

443 Aas, W., Mortier, A., Bowersox, V., Cherian, R., Faluvegi, G., Fagerli, H., Hand, J., Klimont, Z.,

444 Galy-Lacaux, C., Lehmann, C. M. B., Myhre, C. L., Myhre, G., Olivié, D., Sato, K.,

445 Quaas, J., Rao, P. S. P., Schulz, M., Shindell, D., Skeie, R. B., Stein, A., Takemura, T.,

446 Tsyro, S., Vet, R. and Xu, X.: Global and regional trends of atmospheric sulfur, *Sci. Rep.*,

447 9(1), 1–11, doi:10.1038/s41598-018-37304-0, 2019.

448 Abatzoglou, J. T. and Williams, A. P.: Impact of anthropogenic climate change on wildfire

449 across western US forests, *Proc. Natl. Acad. Sci. U. S. A.*, 113(42), 11770–11775,

450 doi:10.1073/pnas.1607171113, 2016.

451 Ahern, A. T., Robinson, E. S., Tkacik, D. S., Saleh, R., Hatch, L. E., Barsanti, K. C., Stockwell,

452 C. E., Yokelson, R. J., Presto, A. A., Robinson, A. L., Sullivan, R. C. and Donahue, N.

453 M.: Production of Secondary Organic Aerosol During Aging of Biomass Burning Smoke

454 From Fresh Fuels and Its Relationship to VOC Precursors, *J. Geophys. Res. Atmos.*,

455 124(6), 3583–3606, doi:10.1029/2018JD029068, 2019.

456 Akagi, S. K., Yokelson, R. J., Wiedinmyer, C., Alvarado, M. J., Reid, J. S., Karl, T., Crouse, J.

457 D. and Wennberg, P. O.: Emission factors for open and domestic biomass burning for use

458 in atmospheric models, *Atmos. Chem. Phys.*, 11(9), 4039–4072, doi:10.5194/acp-11-



- 459 4039-2011, 2011.
- 460 Andreae, M. O.: Emission of trace gases and aerosols from biomass burning – An updated
461 assessment, *Atmos. Chem. Phys.*, 1–27, doi:10.5194/acp-2019-303, 2019.
- 462 Canada’s National Forest Inventory, [online] Available from: <https://nfi.nfis.org/en/> (Accessed
463 18 February 2020), 2020.
- 464 Barbero, R., Abatzoglou, J. T., Larkin, N. K., Kolden, C. A. and Stocks, B.: Climate change
465 presents increased potential for very large fires in the contiguous United States, *Int. J.*
466 *Wildl. Fire*, 24(7), 892–899, doi:10.1071/WF15083, 2015.
- 467 Barnes, I., Hjorth, J. and Mihalopoulos, N.: Dimethyl sulfide and dimethyl sulfoxide and their
468 oxidation in the atmosphere, *Chem. Rev.*, 106(3), 940–975, doi:10.1021/cr020529+,
469 2006.
- 470 Bertrand, A., Stefanelli, G., Jen, C. N., Pieber, S. M., Bruns, E. A., Ni, H., Temime-Roussel, B.,
471 Slowik, J. G., Goldstein, A. H., Haddad, I. El, Baltensperger, U., Prévôt, A. S. H.,
472 Wortham, H. and Marchand, N.: Evolution of the chemical fingerprint of biomass
473 burning organic aerosol during aging, *Atmos. Chem. Phys.*, 18(10), 7607–7624,
474 doi:10.5194/acp-18-7607-2018, 2018.
- 475 Burgos, M. A., Mateos, D., Cachorro, V. E., Toledano, C., de Frutos, A. M., Calle, A.,
476 Herguedas, A. and Marcos, J. L.: An analysis of high fine aerosol loading episodes in
477 north-central Spain in the summer 2013 - Impact of Canadian biomass burning episode
478 and local emissions, *Atmos. Environ.*, doi:10.1016/j.atmosenv.2018.04.024, 2018.
- 479 Buysse, C. E., Kaulfus, A., Nair, U. and Jaffe, D. A.: Relationships between Particulate Matter,
480 Ozone, and Nitrogen Oxides during Urban Smoke Events in the Western US, *Environ.*
481 *Sci. Technol.*, 53(21), 12519–12528, doi:10.1021/acs.est.9b05241, 2019.



- 482 Colarco, P. R., Schoeberl, M. R., Doddridge, B. G., Marufu, L. T., Torres, O. and Welton, E. J.:
483 Transport of smoke from Canadian forest fires to the surface near Washington, D.C.:
484 Injection height, entrainment, and optical properties, *J. Geophys. Res. D Atmos.*, 109(6),
485 1–12, doi:10.1029/2003JD004248, 2004.
- 486 Cottle, P., Strawbridge, K. and McKendry, I.: Long-range transport of Siberian wildfire smoke to
487 British Columbia: Lidar observations and air quality impacts, *Atmos. Environ.*,
488 doi:10.1016/j.atmosenv.2014.03.005, 2014.
- 489 Davidian, J.-C. and Kopriva, S.: Regulation of Sulfate Uptake and Assimilation—the Same or
490 Not the Same?, *Mol. Plant*, 3(2), 314–325, doi:10.1093/MP/SSQ001, 2010.
- 491 DeRieux, W.-S. W., Li, Y., Lin, P., Laskin, J., Laskin, A., Bertram, A. K., Nizkorodov, S. A. and
492 Shiraiwa, M.: Predicting the glass transition temperature and viscosity of secondary
493 organic material using molecular composition, *Atmos. Chem. Phys.*, 18(9), 6331–6351,
494 doi:10.5194/acp-18-6331-2018, 2018.
- 495 Ditto, J. C., Barnes, E. B., Khare, P., Takeuchi, M., Joo, T., Bui, A. A. T., Lee-Taylor, J., Eris,
496 G., Chen, Y., Aumont, B., Jimenez, J. L., Ng, N. L., Griffin, R. J. and Gentner, D. R.: An
497 omnipresent diversity and variability in the chemical composition of atmospheric
498 functionalized organic aerosol, *Commun. Chem.*, 1(1), 75, doi:10.1038/s42004-018-
499 0074-3, 2018.
- 500 Ditto, J. C., Joo, T., Khare, P., Sheu, R., Takeuchi, M., Chen, Y., Xu, W., Bui, A. A. T., Sun, Y.,
501 Ng, N. L. and Gentner, D. R.: Effects of Molecular-Level Compositional Variability in
502 Organic Aerosol on Phase State and Thermodynamic Mixing Behavior, *Environ. Sci.*
503 *Technol.*, 53, 13009–13018, doi:10.1021/acs.est.9b02664, 2019.
- 504 Ditto, J. C., Joo, T., Slade, J. H., Shepson, P. B., Ng, N. L. and Gentner, D. R.: Nontargeted



- 505 Tandem Mass Spectrometry Analysis Reveals Diversity and Variability in Aerosol
506 Functional Groups across Multiple Sites, Seasons, and Times of Day, *Environ. Sci.*
507 *Technol. Lett.*, 7(2), 60–69, doi:10.1021/acs.estlett.9b00702, 2020.
- 508 Donahue, N. M., Epstein, S. A., Pandis, S. N. and Robinson, A. L.: A two-dimensional volatility
509 basis set: 1. organic-aerosol mixing thermodynamics, *Atmos. Chem. Phys.*, 11(7), 3303–
510 3318, doi:10.5194/acp-11-3303-2011, 2011.
- 511 Dreessen, J., Sullivan, J. and Delgado, R.: Observations and impacts of transported Canadian
512 wildfire smoke on ozone and aerosol air quality in the Maryland region on June 9–12,
513 2015, *J. Air Waste Manag. Assoc.*, 66(9), 842–862,
514 doi:10.1080/10962247.2016.1161674, 2016.
- 515 Duporté, G., Parshintsev, J., Barreira, L. M. F., Hartonen, K., Kulmala, M. and Riekkola, M. L.:
516 Nitrogen-Containing Low Volatile Compounds from Pinonaldehyde-Dimethylamine
517 Reaction in the Atmosphere: A Laboratory and Field Study, *Environ. Sci. Technol.*,
518 50(9), 4693–4700, doi:10.1021/acs.est.6b00270, 2016.
- 519 Duporté, G., Riva, M., Parshintsev, J., Heikkinen, E., Barreira, L. M. F., Myllys, N., Heikkinen,
520 L., Hartonen, K., Kulmala, M., Ehn, M. and Riekkola, M. L.: Chemical Characterization
521 of Gas- and Particle-Phase Products from the Ozonolysis of α -Pinene in the Presence of
522 Dimethylamine, *Environ. Sci. Technol.*, 51(10), 5602–5610,
523 doi:10.1021/acs.est.6b06231, 2017.
- 524 Fenn, M. E., Bytnerowicz, A., Schilling, S. L. and Ross, C. S.: Atmospheric deposition of
525 nitrogen, sulfur and base cations in jack pine stands in the Athabasca Oil Sands Region,
526 Alberta, Canada, *Environ. Pollut.*, 196, 497–510, doi:10.1016/j.envpol.2014.08.023,
527 2015.



- 528 Forrister, H., Liu, J., Scheuer, E., Dibb, J., Ziemba, L., Thornhill, K. L., Anderson, B., Diskin,
529 G., Perring, A. E., Schwarz, J. P., Campuzano-Jost, P., Day, D. A., Palm, B. P., Jimenez,
530 J. L., Nenes, A. and Weber, R. J.: Evolution of brown carbon in wildfire plumes,
531 *Geophys. Res. Lett.*, 42, 4623–4630, 2015.
- 532 Forster, C., Wandinger, U., Wotawa, G., James, P., Mattis, I., Althausen, D., Simmonds, P.,
533 O’Doherty, S., Jennings, S. G., Kleefeld, C., Schneider, J., Trickl, T., Kreipl, S., Jäger, H.
534 and Stohl, A.: Transport of boreal forest fire emissions from Canada to Europe, J.
535 *Geophys. Res. Atmos.*, 106(D19), 22887–22906, doi:10.1029/2001JD900115, 2001.
- 536 Gahan, J. and Schmalenberger, A.: The role of bacteria and mycorrhiza in plant sulfur supply,
537 *Front. Plant Sci.*, 5(DEC), 1–7, doi:10.3389/fpls.2014.00723, 2014.
- 538 Garofalo, L. A., Pothier, M. A., Levin, E. J. T., Campos, T., Kreidenweis, S. M. and Farmer, D.
539 K.: Emission and Evolution of Submicron Organic Aerosol in Smoke from Wildfires in
540 the Western United States, *ACS Earth Sp. Chem.*, 3(7), 1237–1247,
541 doi:10.1021/acsearthspacechem.9b00125, 2019.
- 542 Gilman, J. B., Lerner, B. M., Kuster, W. C., Goldan, P. D., Warneke, C., Veres, P. R., Roberts, J.
543 M., De Gouw, J. A., Burling, I. R. and Yokelson, R. J.: Biomass burning emissions and
544 potential air quality impacts of volatile organic compounds and other trace gases from
545 fuels common in the US, *Atmos. Chem. Phys.*, 15(24), 13915–13938, doi:10.5194/acp-
546 15-13915-2015, 2015.
- 547 Hallquist, M., Wenger, J. C., Baltensperger, U., Rudich, Y., Simpson, D., Claeys, M., Dommen,
548 J., Donahue, N. M., George, C., Goldstein, A. H., Hamilton, J. F., Herrmann, H.,
549 Hoffmann, T., Iinuma, Y., Jang, M., Jenkin, M. E., Jimenez, J. L., Kiendler-Scharr, A.,
550 Maenhaut, W., McFiggans, G., Mentel, T. F., Monod, A., Prevot, A. S. H., Seinfeld, J.



- 551 H., Surratt, J. D., Szmigielski, R. and Wildt, J.: The formation, properties and impact of
552 secondary organic aerosol: current and emerging issues, *Atmos. Chem. Phys.*, 9(14),
553 5155–5236, doi:10.5194/acp-9-5155-2009, 2009.
- 554 Hatch, L. E., Luo, W., Pankow, J. F., Yokelson, R. J., Stockwell, C. E. and Barsanti, K. C.:
555 Identification and quantification of gaseous organic compounds emitted from biomass
556 burning using two-dimensional gas chromatography-time-of-flight mass spectrometry,
557 *Atmos. Chem. Phys.*, 15(4), 1865–1899, doi:10.5194/acp-15-1865-2015, 2015.
- 558 Hatch, L. E., Rivas-Ubach, A., Jen, C. N., Lipton, M., Goldstein, A. H. and Barsanti, K. C.:
559 Measurements of I/SVOCs in biomass-burning smoke using solid-phase extraction disks
560 and two-dimensional gas chromatography, *Atmos. Chem. Phys.*, 18(24), 17801–17817,
561 doi:10.5194/acp-18-17801-2018, 2018.
- 562 Hatch, L. E., Jen, C. N., Kreisberg, N. M., Selimovic, V., Yokelson, R. J., Stamatidis, C., York, R.
563 A., Foster, D., Stephens, S. L., Goldstein, A. H. and Barsanti, K. C.: Highly Speciated
564 Measurements of Terpenoids Emitted from Laboratory and Mixed-Conifer Forest
565 Prescribed Fires, *Environ. Sci. Technol.*, 53(16), 9418–9428,
566 doi:10.1021/acs.est.9b02612, 2019.
- 567 Hecobian, A., Liu, Z., Hennigan, C. J., Huey, L. G., Jimenez, J. L., Cubison, M. J., Vay, S.,
568 Diskin, G. S., Sachse, G. W., Wisthaler, A., Mikoviny, T., Weinheimer, A. J., Liao, J.,
569 Knapp, D. J., Wennberg, P. O., Kürten, A., Crounse, J. D., St. Clair, J., Wang, Y. and
570 Weber, R. J.: Comparison of chemical characteristics of 495 biomass burning plumes
571 intercepted by the NASA DC-8 aircraft during the ARCTAS/CARB-2008 field
572 campaign, *Atmos. Chem. Phys.*, 11(24), 13325–13337, doi:10.5194/acp-11-13325-2011,
573 2011.



- 574 Hegg, D. A., Radke, L. F., Hobbs, P. V. and Brock, C. A.: Nitrogen and Sulfur Emissions From
575 The Burning of Forest Products Near Large Urban Areas, *J. Geophys. Res.*, 92, 701–714,
576 1987.
- 577 Hennigan, C. J., Miracolo, M. A., Engelhart, G. J., May, A. A., Presto, A. A., Lee, T., Sullivan,
578 A. P., McMeeking, G. R., Coe, H., Wold, C. E., Hao, W. M., Gilman, J. B., Kuster, W.
579 C., De Gouw, J., Schichtel, B. A., Collett, J. L., Kreidenweis, S. M. and Robinson, A. L.:
580 Chemical and physical transformations of organic aerosol from the photo-oxidation of
581 open biomass burning emissions in an environmental chamber, *Atmos. Chem. Phys.*,
582 11(15), 7669–7686, doi:10.5194/acp-11-7669-2011, 2011.
- 583 Huang, W. Z. and Schoenau, J. J.: Forms, amounts and distribution of carbon, nitrogen,
584 phosphorus and sulfur in a boreal aspen forest soil, *Can. J. Soil Sci.*, 76(3), 373–385,
585 doi:10.4141/cjss96-045, 1996.
- 586 Iinuma, Y., Böge, O. and Herrmann, H.: Methyl-nitrocatechols: Atmospheric tracer compounds
587 for biomass burning secondary organic aerosols, *Environ. Sci. Technol.*, 44(22), 8453–
588 8459, doi:10.1021/es102938a, 2010.
- 589 Jencks, W. P. and Lienhard, G. E.: Thiol Addition to the Carbonyl Group. Equilibria and
590 Kinetics, *J. Am. Chem. Soc.*, 88(17), 3982–3995, doi:10.1021/ja00969a017, 1966.
- 591 Jiang, H., Frie, A. L., Lavi, A., Chen, J. Y., Zhang, H., Bahreini, R. and Lin, Y. H.: Brown
592 Carbon Formation from Nighttime Chemistry of Unsaturated Heterocyclic Volatile
593 Organic Compounds, *Environ. Sci. Technol. Lett.*, 6(3), 184–190,
594 doi:10.1021/acs.estlett.9b00017, 2019.
- 595 Jolly, W. M., Cochrane, M. A., Freeborn, P. H., Holden, Z. A., Brown, T. J., Williamson, G. J.
596 and Bowman, D. M. J. S.: Climate-induced variations in global wildfire danger from



- 597 1979 to 2013, *Nat. Commun.*, 6(May), 1–11, doi:10.1038/ncomms8537, 2015.
- 598 Khare, P., Marcotte, A., Sheu, R., Walsh, A. N., Ditto, J. C. and Gentner, D. R.: Advances in
599 offline approaches for trace measurements of complex organic compound mixtures via
600 soft ionization and high-resolution tandem mass spectrometry, *J. Chromatogr. A*, 1598,
601 163–174, doi:10.1016/j.chroma.2019.03.037, 2019.
- 602 Koss, A. R., Sekimoto, K., Gilman, J. B., Selimovic, V., Coggon, M. M., Zarzana, K. J., Yuan,
603 B., Lerner, B. M., Brown, S. S., Jimenez, J. L., Krechmer, J., Roberts, J. M., Warneke,
604 C., Yokelson, R. J. and De Gouw, J.: Non-methane organic gas emissions from biomass
605 burning: Identification, quantification, and emission factors from PTR-ToF during the
606 FIREX 2016 laboratory experiment, *Atmos. Chem. Phys.*, 18(5), 3299–3319,
607 doi:10.5194/acp-18-3299-2018, 2018.
- 608 Van Krevelen, D. W. and Te Nijenhuis, K.: *Properties of Polymers*, 4th ed., Elsevier,
609 Amsterdam., 2009.
- 610 Landis, M. S., Edgerton, E. S., White, E. M., Wentworth, G. R., Sullivan, A. P. and Dillner, A.
611 M.: The impact of the 2016 Fort McMurray Horse River Wildfire on ambient air
612 pollution levels in the Athabasca Oil Sands Region, Alberta, Canada, *Sci. Total Environ.*,
613 618, 1665–1676, doi:10.1016/j.scitotenv.2017.10.008, 2018.
- 614 Laskin, A., Smith, J. S. and Laskin, J.: Molecular Characterization of Nitrogen-Containing
615 Organic Compounds in Biomass Burning Aerosols Using High-Resolution Mass
616 Spectrometry, *Environ. Sci. Technol.*, 43(10), 3764–3771, doi:10.1021/es803456n, 2009.
- 617 Leustek, T.: Sulfate Metabolism, *Arab. B.*, 1(e0017), 1–16, doi:10.1199/tab.0017, 2002.
- 618 Li, S. M., Leithead, A., Moussa, S. G., Liggio, J., Moran, M. D., Wang, D., Hayden, K.,
619 Darlington, A., Gordon, M., Staebler, R., Makar, P. A., Stroud, C. A., McLaren, R., Liu,



- 620 P. S. K., O'Brien, J., Mittermeier, R. L., Zhang, J., Marson, G., Cober, S. G., Wolde, M.
621 and Wentzell, J. J. B.: Differences between measured and reported volatile organic
622 compound emissions from oil sands facilities in Alberta, Canada, Proc. Natl. Acad. Sci.
623 U. S. A., 114(19), E3756–E3765, doi:10.1073/pnas.1617862114, 2017.
- 624 Li, Y., Pöschl, U. and Shiraiwa, M.: Molecular corridors and parameterizations of volatility in
625 the chemical evolution of organic aerosols, Atmos. Chem. Phys., 16(5), 3327–3344,
626 doi:10.5194/acp-16-3327-2016, 2016.
- 627 Liggio, J., Li, S.-M., Hayden, K., Taha, Y. M., Stroud, C., Darlington, A., Drollette, B. D.,
628 Gordon, M., Lee, P., Liu, P., Leithead, A., Moussa, S. G., Wang, D., O'Brien, J.,
629 Mittermeier, R. L., Brook, J. R., Lu, G., Staebler, R. M., Han, Y., Tokarek, T. W.,
630 Osthoff, H. D., Makar, P. A., Zhang, J., Plata, D. L. and Gentner, D. R.: Oil sands
631 operations as a large source of secondary organic aerosols, Nature, 534,
632 doi:10.1038/nature17646, 2016.
- 633 Liggio, J., Moussa, S. G., Wentzell, J., Darlington, A., Liu, P., Leithead, A., Hayden, K.,
634 O'Brien, J., Mittermeier, R. L., Staebler, R., Wolde, M. and Li, S.-M.: Understanding the
635 primary emissions and secondary formation of gaseous organic acids in the oil sands
636 region of Alberta, Canada, Atmos. Chem. Phys., 17(13), 8411–8427, doi:10.5194/acp-17-
637 8411-2017, 2017.
- 638 Lim, C. Y., Hagan, D. H., Coggon, M. M., Koss, A. R., Sekimoto, K., De Gouw, J., Warneke,
639 C., Cappa, C. D. and Kroll, J. H.: Secondary organic aerosol formation from the
640 laboratory oxidation of biomass burning emissions, Atmos. Chem. Phys., 19(19), 12797–
641 12809, doi:10.5194/acp-19-12797-2019, 2019.
- 642 Lin, P., Yu, J. Z., Engling, G. and Kalberer, M.: Organosulfates in humic-like substance fraction



- 643 isolated from aerosols at seven locations in East Asia: A study by ultra-high-resolution
644 mass spectrometry, *Environ. Sci. Technol.*, 46(24), 13118–13127,
645 doi:10.1021/es303570v, 2012.
- 646 Lin, P., Fleming, L. T., Nizkorodov, S. A., Laskin, J. and Laskin, A.: Comprehensive Molecular
647 Characterization of Atmospheric Brown Carbon by High Resolution Mass Spectrometry
648 with Electrospray and Atmospheric Pressure Photoionization, *Anal. Chem.*, 90(21),
649 12493–12502, doi:10.1021/acs.analchem.8b02177, 2018.
- 650 Liu, J. C., Wilson, A., Mickley, L. J., Dominici, F., Ebisu, K., Wang, Y., Sulprizio, M. P., Peng,
651 R. D., Yue, X., Son, J.-Y., Anderson, G. B. and Bell, M. L.: Wildfire-specific Fine
652 Particulate Matter and Risk of Hospital Admissions in Urban and Rural Counties,
653 *Epidemiology*, 28(1), 77–85, doi:10.1111/mec.13536.Application, 2017.
- 654 Liu, Y., Liggio, J. and Staebler, R.: Reactive uptake of ammonia to secondary organic aerosols:
655 Kinetics of organonitrogen formation, *Atmos. Chem. Phys.*, 15(23), 13569–13584,
656 doi:10.5194/acp-15-13569-2015, 2015.
- 657 Di Lorenzo, R. A., Place, B. K., VandenBoer, T. C. and Young, C. J.: Composition of Size-
658 Resolved Aged Boreal Fire Aerosols: Brown Carbon, Biomass Burning Tracers, and
659 Reduced Nitrogen, *ACS Earth Sp. Chem.*, 2(3), 278–285,
660 doi:10.1021/acsearthspacechem.7b00137, 2018.
- 661 Lowe, A. B.: Thiol-ene “click” reactions and recent applications in polymer and materials
662 synthesis, *Polym. Chem.*, 1(1), 17–36, doi:10.1039/b9py00216b, 2010.
- 663 Makar, P. A., Akingunola, A., Aherne, J., Cole, A. S., Aklilu, Y. A., Zhang, J., Wong, I.,
664 Hayden, K., Li, S. M., Kirk, J., Scott, K., Moran, M. D., Robichaud, A., Cathcart, H.,
665 Baratzedah, P., Pabla, B., Cheung, P., Zheng, Q. and Jeffries, D. S.: Estimates of



- 666 exceedances of critical loads for acidifying deposition in Alberta and Saskatchewan,
667 *Atmos. Chem. Phys.*, 18(13), 9897–9927, doi:10.5194/acp-18-9897-2018, 2018.
- 668 Mashkina, A. V.: Catalytic Synthesis Of Sulfides Sulfoxides and Sulfones, *Sulfur reports*, 10(4),
669 279–388, doi:10.1080/01961779108048759, 1991.
- 670 McLinden, C. A., Fioletov, V., Krotkov, N. A., Li, C., Boersma, K. F. and Adams, C.: A Decade
671 of Change in NO₂ and SO₂ over the Canadian Oil Sands As Seen from Space, *Environ.*
672 *Sci. Technol.*, 50(1), 331–337, doi:10.1021/acs.est.5b04985, 2016.
- 673 Meng, F. R., Bourque, C. P. A., Belczewski, R. F., Whitney, N. J. and Arp, P. A.: Foliage
674 responses of spruce trees to long-term low-grade sulfur dioxide deposition, *Environ.*
675 *Pollut.*, 90(2), 143–152, doi:10.1016/0269-7491(94)00101-I, 1995.
- 676 Nozière, B., Kalberer, M., Claeys, M., Allan, J., D’Anna, B., Decesari, S., Finessi, E., Glasius,
677 M., Grgić, I., Hamilton, J. F., Hoffmann, T., Iinuma, Y., Jaoui, M., Kahnt, A., Kampf, C.
678 J., Kourtschev, I., Maenhaut, W., Marsden, N., Saarikoski, S., Schnelle-Kreis, J., Surratt,
679 J. D., Szidat, S., Szmigielski, R. and Wisthaler, A.: The Molecular Identification of
680 Organic Compounds in the Atmosphere: State of the Art and Challenges, *Chem. Rev.*,
681 115(10), 3919–3983, doi:10.1021/cr5003485, 2015.
- 682 Nyborg, M., Solberg, E. D., Malhi, S. S., Takyi, S., Yeung, P. and Chaudhry, M.: Deposition of
683 anthropogenic sulphur dioxide on soils and resulting soil acidification, *Plant-Soil Interact.*
684 *Low pH*, 147–156, doi:10.1007/978-94-011-3438-5_16, 1991.
- 685 Onda, Y.: Oxidative protein-folding systems in plant cells, *Int. J. Cell Biol.*, 2013,
686 doi:10.1155/2013/585431, 2013.
- 687 Pan, Y. P., Wang, Y. S., Tang, G. Q. and Wu, D.: Spatial distribution and temporal variations of
688 atmospheric sulfur deposition in Northern China: Insights into the potential acidification



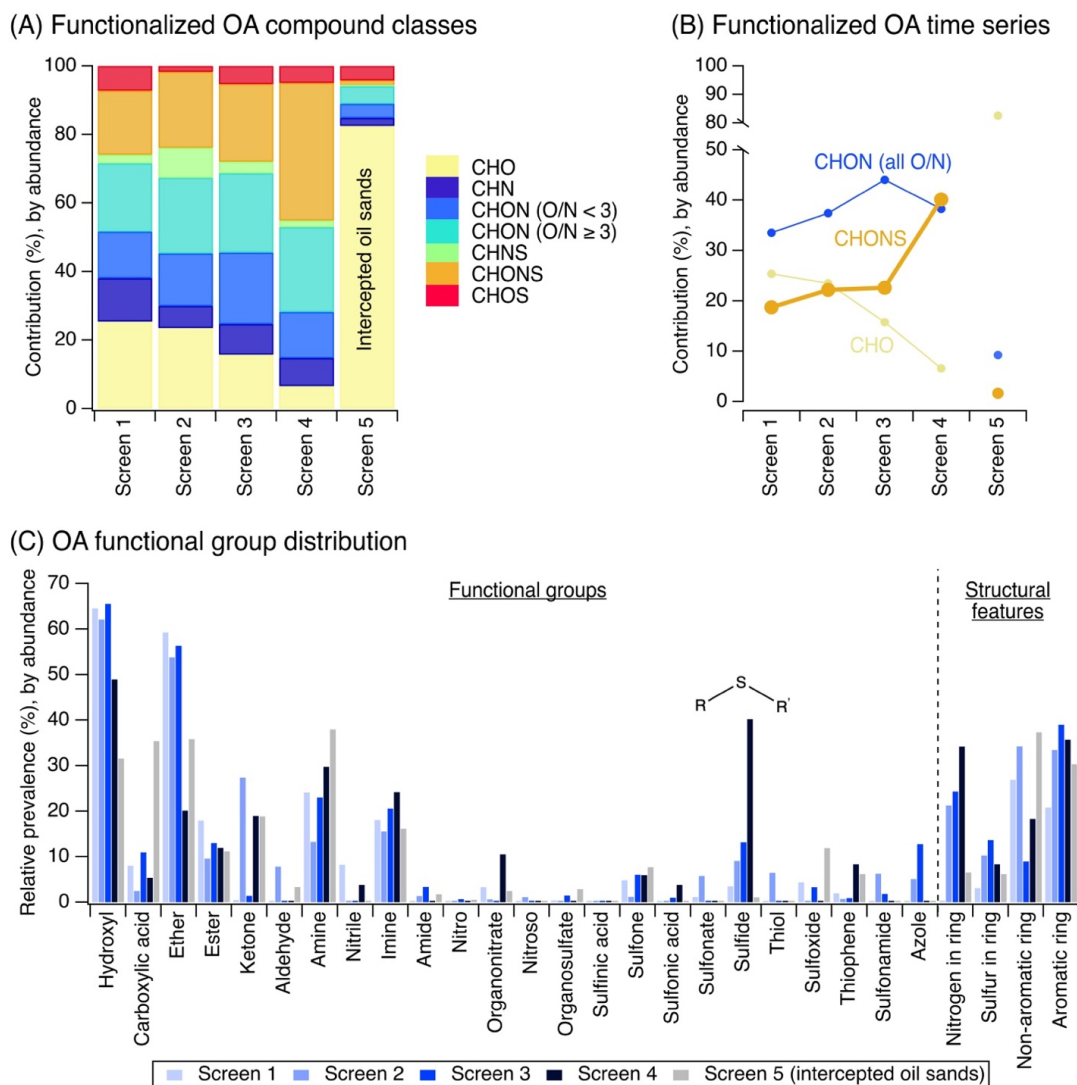
- 689 risks, *Atmos. Chem. Phys.*, 13(3), 1675–1688, doi:10.5194/acp-13-1675-2013, 2013.
- 690 Reid, C. E., Brauer, M., Johnston, F. H., Jerrett, M., Balmes, J. R. and Elliott, C. T.: Critical
691 review of health impacts of wildfire smoke exposure, *Environ. Health Perspect.*, 124(9),
692 1334–1343, doi:10.1289/ehp.1409277, 2016.
- 693 Rogers, H. M., Ditto, J. C. and Gentner, D. R.: Evidence for impacts on surface-level air quality
694 in the northeastern US from long-distance transport of smoke from North American fires
695 during the Long Island Sound Tropospheric Ozone Study (LISTOS) 2018, *Atmos. Chem.*
696 *Phys.*, 20(2), 671–682, doi:10.5194/acp-20-671-2020, 2020.
- 697 Sekimoto, K., Koss, A. R., Gilman, J. B., Selimovic, V., Coggon, M. M., Zarzana, K. J., Yuan,
698 B., Lerner, B. M., Brown, S. S., Warneke, C., Yokelson, R. J., Roberts, J. M. and De
699 Gouw, J.: High-and low-temperature pyrolysis profiles describe volatile organic
700 compound emissions from western US wildfire fuels, *Atmos. Chem. Phys.*, 18(13),
701 9263–9281, doi:10.5194/acp-18-9263-2018, 2018.
- 702 Sengupta, D., Samburova, V., Bhattarai, C., Kirillova, E., Mazzoleni, L., Iaukea-Lum, M., Watts,
703 A., Moosmüller, H. and Khlystov, A.: Light absorption by polar and non-polar aerosol
704 compounds from laboratory biomass combustion, *Atmos. Chem. Phys.*, 18(15), 10849–
705 10867, doi:10.5194/acp-18-10849-2018, 2018.
- 706 Sheu, R., Marcotte, A., Khare, P., Charan, S., Ditto, J. C. and Gentner, D. R.: Advances in
707 offline approaches for chemically speciated measurements of trace gas-phase organic
708 compounds via adsorbent tubes in an integrated sampling-to-analysis system, *J.*
709 *Chromatogr. A*, 1575, 80–90, doi:10.1016/j.chroma.2018.09.014, 2018.
- 710 Song, J., Li, M., Fan, X., Zou, C., Zhu, M., Jiang, B., Yu, Z., Jia, W., Liao, Y. and Peng, P.:
711 Molecular Characterization of Water- And Methanol-Soluble Organic Compounds



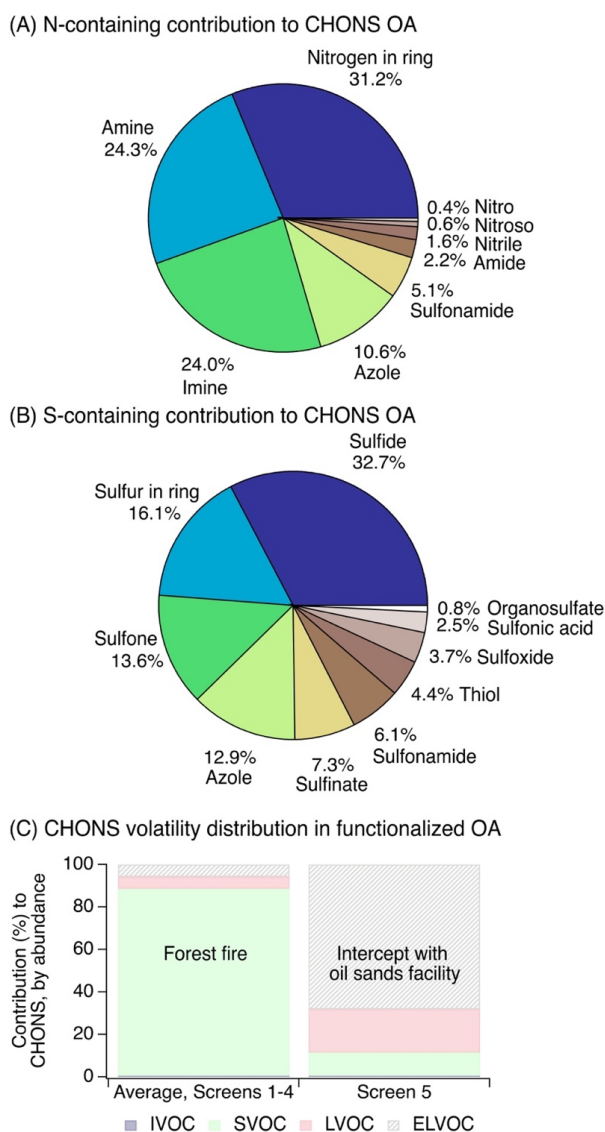
- 712 Emitted from Residential Coal Combustion Using Ultrahigh-Resolution Electrospray
713 Ionization Fourier Transform Ion Cyclotron Resonance Mass Spectrometry, *Environ. Sci.*
714 *Technol.*, 53(23), 13607–13617, doi:10.1021/acs.est.9b04331, 2019.
- 715 Updyke, K. M., Nguyen, T. B. and Nizkorodov, S. A.: Formation of brown carbon via reactions
716 of ammonia with secondary organic aerosols from biogenic and anthropogenic
717 precursors, *Atmos. Environ.*, 63, 22–31, doi:10.1016/j.atmosenv.2012.09.012, 2012.
- 718 Val Martín, M., Honrath, R. E., Owen, R. C., Pfister, G., Fialho, P. and Barata, F.: Significant
719 enhancements of nitrogen oxides, black carbon, and ozone in the North Atlantic lower
720 free troposphere resulting from North American boreal wildfires, *J. Geophys. Res.*
721 *Atmos.*, 111(23), 1–17, doi:10.1029/2006JD007530, 2006.
- 722 Vicente, A., Alves, C., Calvo, A. I., Fernandes, A. P., Nunes, T., Monteiro, C., Almeida, S. M.
723 and Pio, C.: Emission factors and detailed chemical composition of smoke particles from
724 the 2010 wildfire season, *Atmos. Environ.*, doi:10.1016/j.atmosenv.2013.01.062, 2013.
- 725 Wang, X., Wang, H., Jing, H., Wang, W. N., Cui, W., Williams, B. J. and Biswas, P.: Formation
726 of Nitrogen-Containing Organic Aerosol during Combustion of High-Sulfur-Content
727 Coal, *Energy and Fuels*, 31(12), 14161–14168, doi:10.1021/acs.energyfuels.7b02273,
728 2017a.
- 729 Wang, X. K., Rossignol, S., Ma, Y., Yao, L., Wang, M. Y., Chen, J. M., George, C. and Wang,
730 L.: Molecular characterization of atmospheric particulate organosulfates in three
731 megacities at the middle and lower reaches of the Yangtze River, *Atmos. Chem. Phys.*,
732 16(4), 2285–2298, doi:10.5194/acp-16-2285-2016, 2016.
- 733 Wang, X. K., Hayeck, N., Brüggemann, M., Yao, L., Chen, H., Zhang, C., Emmelin, C., Chen,
734 J., George, C. and Wang, L.: Chemical Characteristics of Organic Aerosols in Shanghai:



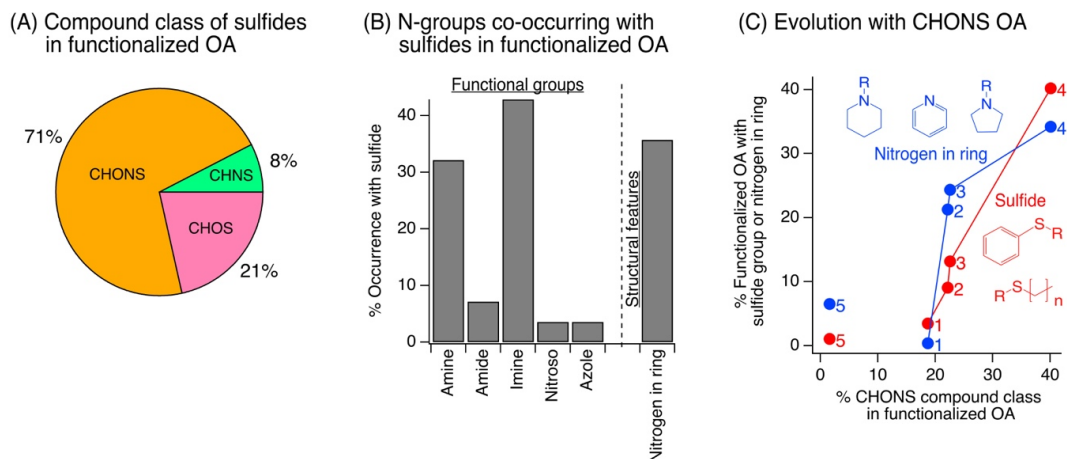
- 735 A Study by Ultrahigh-Performance Liquid Chromatography Coupled With Orbitrap Mass
736 Spectrometry, *J. Geophys. Res. Atmos.*, 122(21), 11,703-11,722,
737 doi:10.1002/2017JD026930, 2017b.
- 738 Ward, D. E.: Factors Influencing the Emissions of Gases and Particulate Matter from Biomass
739 Burning, in *Fire in the Tropical Biota: Ecosystem Processes and Global Challenges*, pp.
740 418–436., 1990.
- 741 Wong, J. P. S., Tsagkaraki, M., Tsiodra, I., Mihalopoulos, N., Violaki, K., Kanakidou, M.,
742 Sciare, J., Nenes, A. and Weber, R. J.: Effects of Atmospheric Processing on the
743 Oxidative Potential of Biomass Burning Organic Aerosols, *Environ. Sci. Technol.*,
744 53(12), 6747–6756, doi:10.1021/acs.est.9b01034, 2019.
- 745 Yokelson, R. J., Burling, I. R., Gilman, J. B., Warneke, C., Stockwell, C. E., De Gouw, J., Akagi,
746 S. K., Urbanski, S. P., Veres, P., Roberts, J. M., Kuster, W. C., Reardon, J., Griffith, D.
747 W. T., Johnson, T. J., Hosseini, S., Miller, J. W., Cocker, D. R., Jung, H. and Weise, D.
748 R.: Coupling field and laboratory measurements to estimate the emission factors of
749 identified and unidentified trace gases for prescribed fires, *Atmos. Chem. Phys.*, 13(1),
750 89–116, doi:10.5194/acp-13-89-2013, 2013.



751 **Figure 1.** (A) The compound class distribution of functionalized OA (from non-targeted LC-ESI-MS) weighted by ion abundance, shown as percent contribution of each compound class to the total compound abundance measured by LC-ESI-MS. (B) Percent contribution of CHO, 752 CHON, and CHONS compound classes in functionalized OA as a function of plume age. CHON 753 compounds in panel B are summed across all O/N ratios. (C) Functional groups and structural 754 features present in measured functionalized OA (from non-targeted LC-ESI-MS/MS). The 755 sulfide functional group is shown here for emphasis, and will be the subject of subsequent 756 analyses. For panels A-C, results tabulated by occurrence and absolute ion abundance are shown 757 in Figure S5-S6, and functional group tallying methods are discussed in Supporting Information 758 S3. 759 760



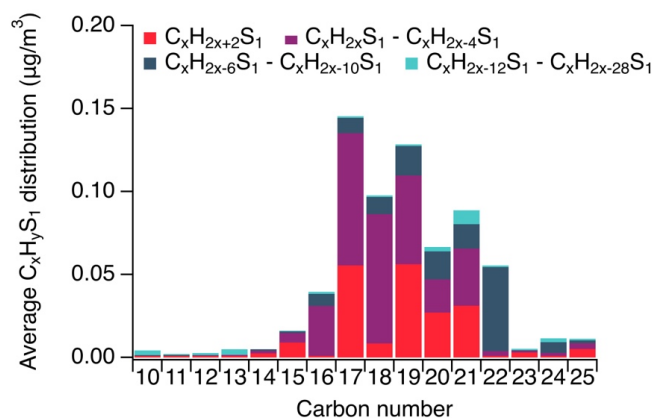
761 **Figure 2.** (A) The observed particle-phase CHONS compounds included cyclic nitrogen and a
762 range of N-containing functional groups (organonitrates are excluded here due to challenges with
763 their identification using SIRIUS with CSI:FingerID, but contributed minimally to CHONS,
764 Supporting Information S3). (B) These CHONS compounds showed a variety of S-containing
765 functional groups with sulfides being the most prominent. For panels A-B, data are averaged
766 across screens 1-4, with individual screens shown in Figure S7A. (C) The particle-phase CHONS
767 compounds formed in the forest fire plume were mostly SVOCs. These volatility data were
768 averaged across screens 1-4, and individual screens are shown in Figure S8. Volatility was
769 estimated with the parameterization in Li et al. (Li et al., 2016) and grouped according to
770 volatility bins in Donahue et al. (Donahue et al., 2011).



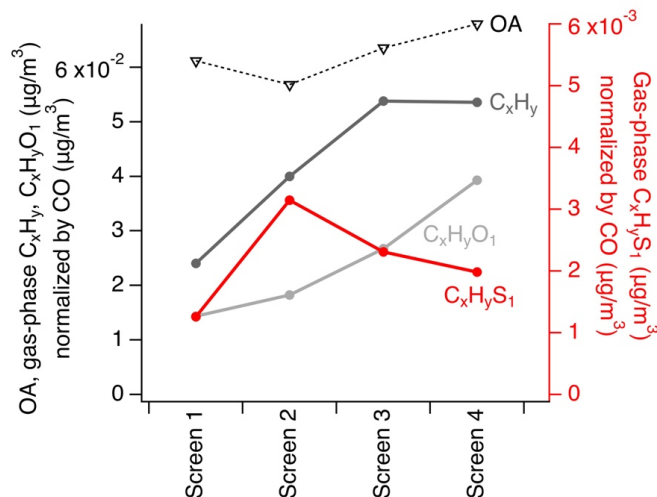
771 **Figure 3.** (A) 71% of sulfide functional groups observed (weighted by ion abundance) were
772 present in CHONS compounds. (B) Sulfides were often paired with amines, imines, and cyclic
773 nitrogen features. Data shown in panels A-B are cumulative across compounds in screens 1-4.
774 (C) The relative contribution of sulfides and cyclic nitrogen groups to all functionalized OA
775 increased together with the increasing contribution of CHONS compounds. The other functional
776 groups shown in panel B showed no relationship with the increase in CHONS (Figure S7B).
777 Structures represent examples of commonly observed sulfide and cyclic nitrogen substructures
778 from SIRIUS and CSI:FingerID (Supporting Information S3), where ring structures associated
779 with nitrogen heteroatoms were free standing, adjacent to other rings, and/or contained additional
780 attached functional groups.



(A) Average gas-phase $C_xH_yS_1$ distribution



(B) Gas-phase and AMS OA concentrations normalized by CO



781 **Figure 4.** (A) The average $C_xH_yS_1$ distribution from targeted GC-APCI-MS across all samples
782 from screens 1-4 (see Figure S10 for individual $C_xH_yS_1$ screens, and Figure S13 for C_xH_y). (B)
783 Concentrations of gas-phase C_xH_y , $C_xH_yO_1$, $C_xH_yS_1$ from targeted GC-APCI-MS, and total OA
784 from AMS, all normalized by carbon monoxide concentration across screens 1-4 (see Figure
785 S12A for non-normalized concentrations). Data in panel B are averaged over low and high
786 altitude adsorbent tube samples.